International Journal of Applied Earth Observation and Geoinformation 136 (2025) 104390

Contents lists available at ScienceDirect

International Journal of Applied Earth Observation and Geoinformation

journal homepage: www.elsevier.com/locate/jag

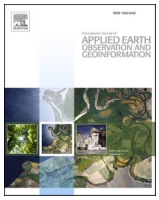

Predicting turbidity dynamics in small reservoirs in central Kenya using remote sensing and machine learning

Stefanie Steinbach [a,b,*], Anna Bartels [b], Andreas Rienow [b], Bartholomew Thiong'o Kuria [c], Sander Jaap Zwart [d], Andrew Nelson [a]

[a] Faculty of Geo-Information Science and Earth Observation (ITC), University of Twente, Enschede, The Netherlands
[b] Institute of Geography, Ruhr University Bochum, Bochum, Germany
[c] Institute of Geomatics, GIS and Remote Sensing (IGGReS), Dedan Kimathi University of Technology, Nyeri, Kenya
[d] International Water Management Institute (IWMI), Accra, Ghana

ARTICLE INFO

Keywords:
Sentinel-2
Water quality
Turbidity
Agricultural water management

ABSTRACT

Small reservoirs are increasingly common across Africa. They provide decentralised access to water and support farmer-led irrigation, in addition to contributing towards mitigating the impacts of climate change. Water quality monitoring is essential to ensure the safe use of water and to understand the impact of the environment and land use on water quality. However, water quality in small reservoirs is often not monitored continuously, with the interlinkages between weather, land, and water remaining unknown. Turbidity is a prime indicator of water quality that can be assessed with remote sensing techniques. Here we modelled turbidity in 34 small reservoirs in central Kenya with Sentinel-2 data from 2017 to 2023 and predicted turbidity outcomes using primary and secondary Earth observation data, and machine learning. We found distinct monthly turbidity patterns. Random forest and gradient boosting models showed that annual turbidity outcomes depend on meteorological variables, topography, and land cover ($R^2 = 0.46$ and 0.43 respectively), while longer-term turbidity was influenced more strongly by land management and land cover ($R^2 = 0.88$ and 0.72 respectively). Our results suggest that short- and longer-term turbidity prediction can inform reservoir siting and management. However, inter-annual variability prediction could benefit from more knowledge of additional factors that may not be fully captured in commonly available geospatial data. This study contributes to the relatively small body of remote sensing-based research on water quality in small reservoirs and supports improved small-scale water management.

1. Introduction

Turbidity, a measure of water cloudiness from organic and inorganic particles, is a prime indicator of water quality. High turbidity levels negatively impact aquatic ecology and human use directly and indirectly (Davies-Colley and Smith, 2001). Pathogens can adhere to suspended particles and generally co-occur with other pollutants, which is a risk factor for human and livestock water consumption (De Troyer et al., 2016). Decreased sight can cause behavioural and reproductive alterations in fish and other organisms (Henley et al., 2000). Irrigation water with high particle load can decrease the lifespan of equipment and damage crops (Müller and Cornel, 2017). Small reservoirs < 100 ha are extremely common in sub-Saharan Africa (SSA) (Kibret et al., 2021). They are multi-purpose water sources, that provide decentralised water access, contribute to climate change mitigation, farmer-led irrigation, and fishing and aquaculture, and thus to water and food security, particularly in rural areas (Saruchera and Lautze, 2019). Therefore, regular monitoring and control of turbidity levels is essential for safe and effective water use.

Modelling water quality parameters, such as turbidity, from satellite imagery allows for efficient and continuous data retrieval, which can capture variability at different spatial and temporal scales (Dörnhöfer and Oppelt, 2016; Warren et al., 2021). This is particularly useful for small water bodies, which are generally underrepresented in water quality monitoring networks (Winton et al., 2019). The availability of openly accessible high spatial resolution satellite imagery, such as of the Copernicus missions' Sentinel-2 satellites, provides unprecedented opportunities for detecting and monitoring small water bodies (Papa et al., 2023). Several studies have leveraged this for mapping their locations and dynamics in different areas across Africa (Bangira et al., 2019;

* Corresponding author.
E-mail addresses: s.steinbach@utwente.nl, stefanie.steinbach@rub.de (S. Steinbach).

https://doi.org/10.1016/j.jag.2025.104390
Received 15 July 2024; Received in revised form 3 December 2024; Accepted 24 January 2025
Available online 6 February 2025

Bhaga et al., 2023; Ghansah et al., 2022). Others have modelled turbidity, or the related indicator suspended sediment (Total Suspended Sediment [TSM] or Suspended Particulate Matter [SPM]), in one or few larger lakes or reservoirs (Kowe et al., 2023; Masocha et al., 2018; Ndou, 2023; Robert et al., 2016). Yet only a few studies have covered small water body turbidity. Robert et al. (2016) modelled SPM in water bodies of several sizes, including smaller ponds, in the Gourma region in Mali with Moderate-resolution Imaging Spectroradiometer (MODIS) and Landsat imagery, and underscored possible improvements to their approach through higher spatial resolution satellite imagery. Cecchi et al. (2020) investigated small reservoirs in Burkina Faso, but used satellite imagery to create land cover maps while assessing SPM based on in-situ measurements.

Previous studies have reported that meteorological variables, land cover and land management, topography, and socio-economic factors can be major drivers of turbidity in lakes and reservoirs (Lin et al., 2023; Liu et al., 2020; Martins et al., 2019; Wang et al., 2021). However, where studies have included small water bodies, they may still be defined as large as $< 100\ km^2$ (e.g. Lin et al., 2023). Larger water bodies may show more distinct seasonal turbidity patterns and clearer reactions to driving forces. In contrast, Gardelle et al. (2010) and Robert et al. (2017) show that small water bodies can exhibit paradoxical behaviour, such as an increase in water levels after drought periods, and have sometimes erratic, complex inter-seasonal and inter-annual turbidity dynamics that overlay and interact with each other.

In East Africa, small reservoirs are often constructed in agriculturally developed wetlands and used as a common water supply strategy (Nakawuka et al., 2018; Uwimana et al., 2018). Understanding and predicting turbidity are both key to site selection, monitoring, and efficiently managing such reservoirs. To fill the gaps in understanding turbidity in small reservoirs in SSA, we address the question of which main factors drive turbidity patterns. This study aims to (1) model turbidity dynamics in 34 small reservoirs located in wetlands in central Kenya based on a Sentinel-2 time series, (2) identify the most important predictors that influence turbidity in the reservoirs, and (3) quantify the relationship between predictors and turbidity. This can help find the most effective management options for reducing turbidity in small reservoirs and contribute to more sustainable water use.

2. Study area

This study covers 34 small wetland reservoirs and their catchments in central Kenya (Fig. 1). They are located between Mount Kenya in the east and the Aberdare Mountain range in the west. Clusters can be grouped into north (Group N) and south (Group S) of 0.3°S. Group N is located on higher grounds, with less vegetation, less built-up area, and

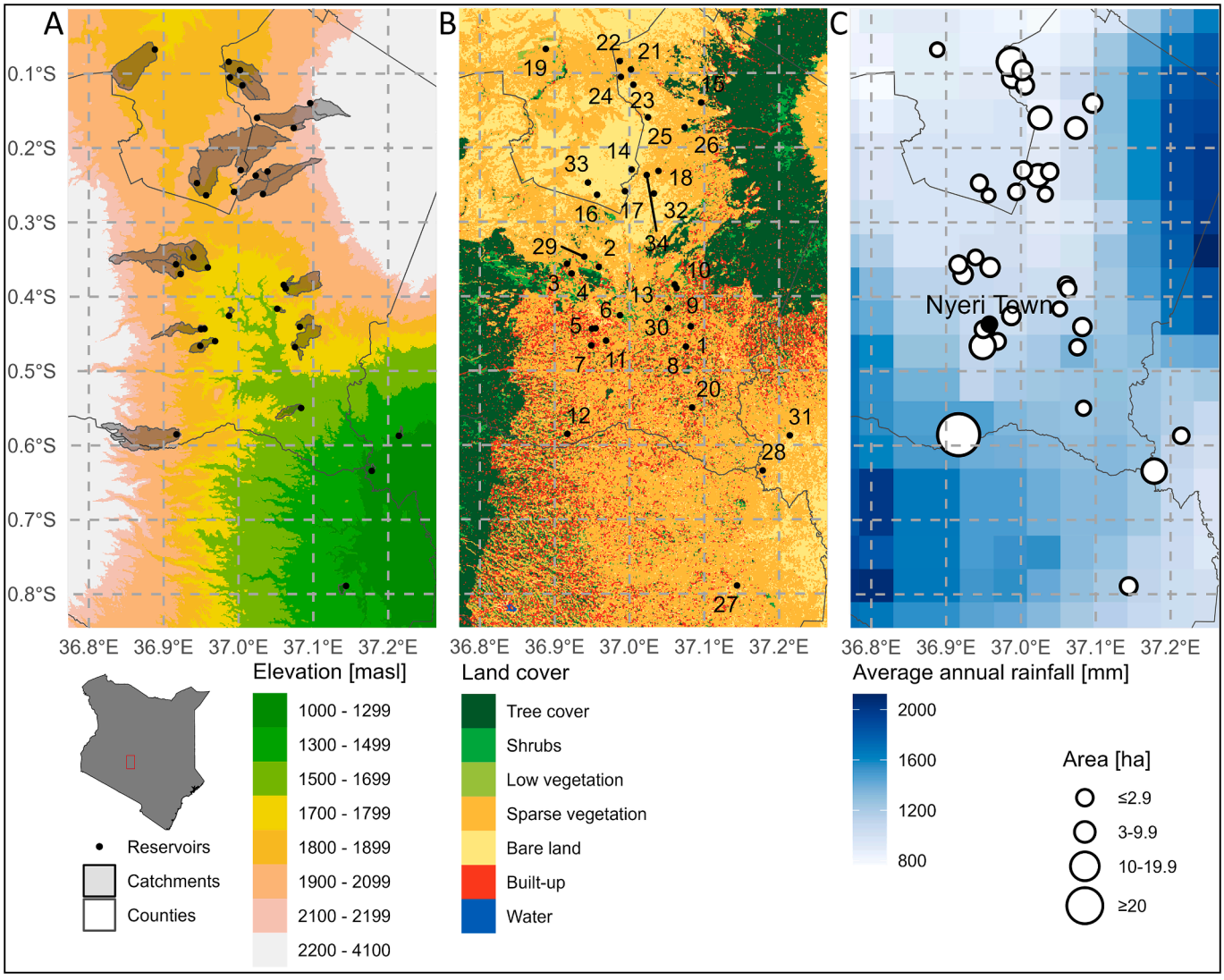

Fig. 1. Overview of the 34 reservoirs with A catchments and topography, B reservoirs with their IDs and land cover, and C reservoir sizes and average annual rainfall. Data sources as given in Section 3.

lower rainfall levels. The bimodal rainfall pattern comprises long rains from March to May and short rains between September and early January (Nathan et al., 2020). The studied reservoirs have surface areas < 21 ha and are used for irrigation, fishing, ecotourism, recreation, livestock watering, and industrial processing (mainly coffee) (WRUA, 2018; Steinbach et al., 2024). Substantial land conversion to cropland has taken place over the past 30 years (Muthee et al., 2022). Current land management practices result in soil erosion and subsequently reservoir siltation has become a problem in the Upper Tana basin, with a hotspot around Nyeri town (Kauffman et al., 2014). The Kenya Bureau of Standards (KEBS) defines standards for water quality parameters, with a turbidity limit < 25 nephelometric turbidity units (NTU) for natural potable water (KEBS, 2015). However, the local Muringato Water Resource User Association (WRUA) identified a lack of information on water resources that impedes their informed management (WRUA, 2018).

3. Methods

Fig. 2 depicts the workflow. To assess turbidity dynamics from 2017 to 2023, we modelled turbidity for all 34 reservoirs (Section 3.1), selected possible predictors (Section 3.2), and used machine learning (ML) to identify the most important predictors, derive median model accuracies across multiple iterations, and quantify the relationship

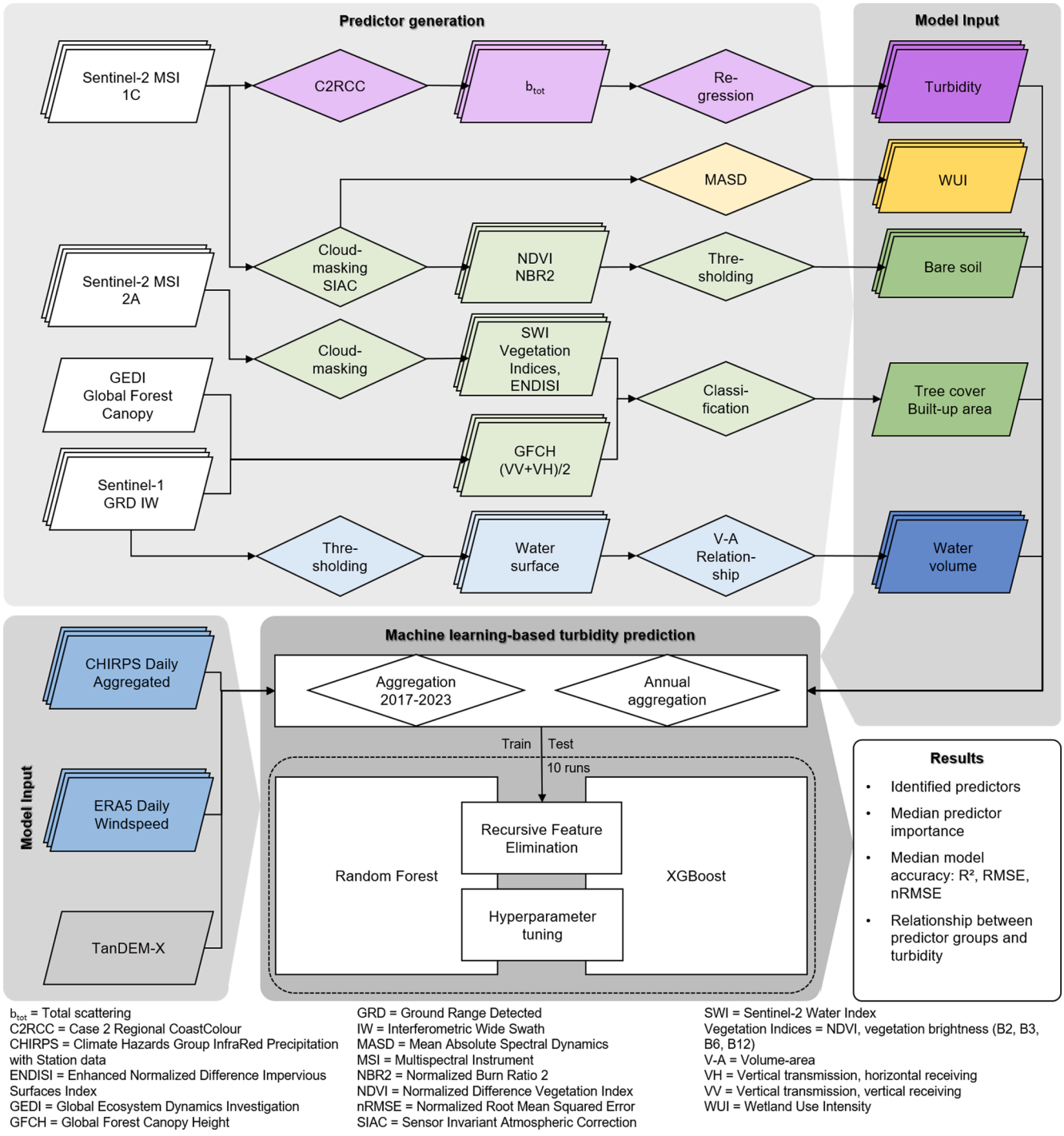

b_{tot} = Total scattering
C2RCC = Case 2 Regional CoastColour
CHIRPS = Climate Hazards Group InfraRed Precipitation with Station data
ENDISI = Enhanced Normalized Difference Impervious Surfaces Index
GEDI = Global Ecosystem Dynamics Investigation
GFCH = Global Forest Canopy Height
GRD = Ground Range Detected
IW = Interferometric Wide Swath
MASD = Mean Absolute Spectral Dynamics
MSI = Multispectral Instrument
NBR2 = Normalized Burn Ratio 2
NDVI = Normalized Difference Vegetation Index
nRMSE = Normalized Root Mean Squared Error
SIAC = Sensor Invariant Atmospheric Correction
SWI = Sentinel-2 Water Index
Vegetation Indices = NDVI, vegetation brightness (B2, B3, B6, B12)
V-A = Volume-area
VH = Vertical transmission, horizontal receiving
VV = Vertical transmission, vertical receiving
WUI = Wetland Use Intensity

Fig. 2. Workflow for turbidity assessment and modelling.

between predictor groups and inter-annual and multi-year turbidity outcomes (Section 3.3).

3.1. Modelling turbidity from satellite observations

We modelled turbidity using a time series of Sentinel-2 Level-1C (1C) data from the multispectral instrument (MSI) (tile MBV) from 2017 to 2023. All images below a cloud threshold of 40 % were downloaded from the Copernicus Dataspace (dataspace.copernicus.eu). We used the Case 2 Regional CoastColour (C2RCC) processor (Brockmann et al., 2016) in the Sentinel Applications Platform (SNAP) 9.0 and automated the workflow with its Python implementation snappy (ESA, 2022). C2RCC was developed for atmospheric correction over water and uses neural networks to invert a large database of radiative transfer simulations to retrieve optically active constituents (inherent optical properties, IOP), from which turbidity can be inferred (Brockmann et al., 2016). C2RCC requires ancillary data for atmospheric correction. For that, we averaged the reservoirs' elevation from the TanDEM-X digital elevation model (DEM), set salinity to 0, generated average air pressure and temperature from the National Centers for Environmental Prediction (NCEP) and National Center for Atmospheric Research (NCAR) Reanalysis Project, and used average ozone concentration from the Total Ozone Mapping Spectrometer (TOMS) products. The NCEP/NCAR and TOMS products are available in the Google Earth Engine catalogue (GEE) (Gorelick et al., 2017).

We used the parameters from Steinbach et al. (2024), who parameterized the model for 10 of the studied reservoirs using 45 in-situ measurements in January 2023 ($R^2 = 0.83$). The model

$$Turbidity = 0.66 * {b_{tot}}^{1.13} \quad (1)$$

uses the IOP b_{tot}. It is the sum of b_{part}, typical sediment scattering, and b_{wit}, white scatterer that are the output from the C2X-COMPLEX neural networks in C2RCC, which are trained for optically complex inland waters (Soriano-González et al., 2022). Turbidity was extracted as the average within a 3 × 3-pixel radius at a central location in the reservoir. Considering that with water table variations, reservoirs do not necessarily shrink concentrically, the point for value extraction was set within the centre of the smallest 25 % of the generated water polygons. The values were averaged per month to create a regular time series.

3.2. Predictor variables

The predictor variables were identified from published literature based on dominant biological and physical processes that influence turbidity in water bodies. The predictor groups include surface water-related predictors, meteorological predictors, topography, vegetation and bare soil, land cover and management (Table 1).

The size of a water body can be related to effects of dilution, buffer capacity, and resuspension of bottom sediment from wind (Wang et al., 2021). We created a time series of surface water occurrence from all available Sentinel-1 Ground Range Detected (GRD) ascending scenes in Interferometric Wide Swath (IW) mode by applying Otsu thresholding (Otsu, 1979). Water volume was estimated as

$$V = aA^b \quad (2)$$

where V is the volume, A is the surface area, and a and b are scaling coefficients (Vanthof and Kelly, 2019). We optimised these coefficients through a regression of surface water occurrence estimation on January 19, 2023, and volume based on bathymetric measurements from ten reservoirs taken between January 8 and 27, 2023 ($R^2 = 0.98$). Due to singular downward outliers, the regular time series was created using monthly maxima. Remaining outliers were removed using the Median Absolute Deviation (MAD) about the median in a rolling window (Hampel, 1974).

Rainfall can both lead to dilution of suspended sediment and to increased sediment input from water erosion (Lacour et al., 2009). Wind leads to aeolian sediment input and internal sediment resuspension (Wang et al., 2021; Zhang et al., 2022). We selected the Climate Hazards Group InfraRed Precipitation with Station data (CHIRPS) daily rainfall data (Funk et al., 2015) and the daily ERA5-Land Daily Aggregates dataset (Copernicus Climate Change Service, 2019). Data availability and the spatial resolution of 0.05° and 0.1°, respectively, guided this choice. For rainfall as a hydrological component, we used sum and maximum per catchment, and for wind mean and maximum speeds at the reservoir. For absolute windspeed, we applied

$$ws = \sqrt{u^2 + v^2} \quad (3)$$

where ws is windspeed while u and v represent the eastward and northward components. As steeper slopes can enhance the effect of

Table 1
Candidate predictors of small reservoir turbidity.

	Predictor	Metric	Spatial reference	Dataset	Reference
Surface water-related	Water volume	Mean	Reservoir	Sentinel-1 IW GRD, sonar measurements	(Steinbach et al., 2021; Vanthof and Kelly, 2019)
Land cover	% bare soil	Mean	Catchment, 5 km & 50 m buffers	Sentinel-2 MSI 1C	(Urbina-Salazar et al., 2023)
	NDVI	Mean	Catchment, 5 km & 50 m buffers	Sentinel-2 MSI 1C	(Tucker, 1979)
	% forested*		Catchment, 5 km & 50 m buffers	Sentinel-2 MSI 2A GEDI	(Goebel et al., 2023)
	% built-up*		Catchment, 5 km & 50 m buffers	Sentinel-2 MSI 2A GEDI	(Goebel et al., 2023)
Meteorological	Rainfall	Sum & Maximum	Catchment	CHIRPS Daily	(Funk et al., 2015)
	Absolute wind speed	Mean & Maximum	Reservoir	ERA5-Land Daily Aggregated	(Copernicus Climate Change Service, 2019)
Land management	Wetland Use Intensity (WUI)	Mean	Catchment, 5 km & 50 m buffers	Sentinel-2 MSI 1C	(Steinbach et al., 2023)
Topography	Slope	Mean	Catchment	TanDEM-X DEM	(Rizzoli et al., 2017)

*Only for the long-term analysis.

rainfall with stronger runoff, erosion, and sediment input (Defersha and Melesse, 2012), slope was calculated from the TanDEM-X DEM with a spatial resolution of 12 m (Rizzoli et al., 2017).

Forested areas tend to decrease turbidity, while bare soil and built-up areas increase turbidity due to higher rates of erosion and runoff (Cecchi et al., 2020; De Troyer et al., 2016; Locke, 2024; Robert et al., 2016; Shen et al., 2022). Therefore, we created monthly time series of vegetation and bare soil fraction from Sentinel-2 Level-1C time series. We used the 1C processing level because Sentinel-2 surface reflectance data on GEE was not available for the entire observation period for the study area. We then ran the Sensor Invariant Atmospheric Correction (SIAC) on GEE (Yin et al., 2022) to atmospherically correct all scenes < 40 % cloud cover, and cloud-masked the time series as described by Goebel et al. (2023). Then, we calculated the normalised difference vegetation index (NDVI) (Tucker, 1979) and classified bare soil by applying thresholds to NDVI and normalized burn ratio 2 (NBR2), following Urbina-Salazar et al. (2023). We visually evaluated the result with the bare soil extent of the land cover classification of part of the study area by Goebel et al. (2023). We extracted built-up and forest area by extending the same land cover classification for the 2019 dry season to cover the study area. The object-based sequential classification approach is tailored to heterogeneous landscapes by focusing on evaluating image objects based on their homogeneity in terms of optical and backscatter properties, and Global Ecosystem Dynamics Investigation (GEDI) canopy height (Potapov et al., 2021). To add an additional dimension of land cover variability and intensity of use, annual Wetland Use Intensity (WUI), a measure of cumulative reflectance change between time steps, was created from monthly mosaics (Steinbach et al., 2023) that we generated from SIAC-corrected Sentinel-2 images with < 40 % cloud cover.

Two spatial and two temporal aggregation approaches were considered. Cecchi et al. (2020) show that catchment-based predictors and predictors in a 5 km buffer contributed differently to turbidity trends. Accordingly, we calculated land cover and management predictors at both scales. We added a 50 m buffer to account for riparian vegetation, which can filter sediment input (Mwaura, 2006). We aggregated the regular time series to annual and overall metrics. Due to gaps in the turbidity time series from cloud cover and water cover variations, to avoid bias, observations with < 25 % valid data points per single year or across all years, respectively, were discarded. This resulted in 186 observations for the annual dataset and 29 observations for the time series aggregated across all years.

3.3. Machine learning-based predictor selection

To assess how the predictors influence turbidity, we used random forest (RF) regression and gradient-boosting with recursive feature elimination (RFE) in R (R Core Team, 2024). Both are ML algorithms that are based on ensembles of decision trees. For RF, the regression result is the average across single decision trees trained on bootstrap samples from a random predictor subset at each split (Breiman, 2001). The gradient-boosting tree algorithm eXtreme Gradient Boosting (XGBoost) is a resource-efficient method that arranges trees sequentially, where new trees learn from previous ones (Chen et al., 2024). Ensemble ML algorithms are widely used in environmental modelling as they can model more complex relationships between predictors and response variables than classical statistical methods at high accuracies. At the same time, they require less training data than deep learning-based approaches, making them suitable for the present scenario (Pichler and Hartig, 2023; Sagan et al., 2020). Hyperparameter tuning served to optimise the models, and the best performing models were selected. RFE is a popular feature elimination method that starts with the whole predictor set and iteratively removes the least important ones until a minimal dataset is reached (Díaz-Uriarte and Alvarez De Andrés, 2006). RF and XGBoost were used to model average turbidity for each year and average turbidity across all years. The coefficient of determination R^2, root mean squared error (RMSE), and normalised RMSE (nRMSE) indicated model performance. For improved model robustness, we applied 10 replications and calculated median variable importances and accuracy metrics. Table 2 summarises the approaches and values.

4. Results

4.1. Spatio-temporal turbidity dynamics

All the reservoirs in the study area exhibit elevated turbidity levels beyond 25 NTU at some point during the observation period. However, we observed distinct patterns in Group N and Group S (Fig. 3). Group N reservoirs have overall higher average values of 89.7 NTU (median = 71.9 NTU) compared to 28 NTU (median = 11.8 NTU) in Group S. They exceeded the level more regularly, between 33 % and 100 % of the months with valid observations as opposed to 2–65 % for Group S (Fig. 3B). Fig. 3C shows boxplots of the aggregated monthly values in both groups. In March and July, they showed contrasting behaviour with particularly high (mean = 122 NTU and 112 NTU, median = 102 NTU and 79 NTU) and markedly low turbidity (mean = 26 NTU and 20 NTU, median = 12 NTU and 7 NTU), respectively. The Wilcoxon rank-sum test confirmed that the difference between the groups was significant for each month ($p = 0.01$).

4.2. Variables influencing turbidity

The results of the RF and XGBoost models with RFE-based predictor selection and hyperparameter tuning are displayed in Fig. 4. Interannual turbidity variability was explained with higher accuracy by RF ($R^2 = 0.46$ and $R^2 = 0.88$) than by XGBoost ($R^2 = 0.43$ and $R^2 = 0.72$). Median variable importances for the annual analysis (Fig. 4A, B) and for the overall aggregation (Fig. 4C, D), had comparable patterns. For interannual variability, meteorological predictors had the largest share (RF: 43.3 %, XGBoost: 56.7 %), with maximum windspeed showing the highest importance in both models, before the topographic predictor mean slope (RF: 15.0 %, XGBoost: 24.4 %), followed by water volume, land cover, and other meteorological variables. The aggregated share of land management predictors was smaller than that of land cover for both models, with 10.8 % and 25.0 % for RF, and 0.8 % and 8.5 % for XGBoost.

In contrast, for the models explaining overall turbidity variability,

Table 2
Machine learning regression, feature selection, and accuracy assessment approaches.

Approach	(Hyper-) Parameter	Description	Values	R Package
RF	ntree	Number of trees	[100, 500, 1000]	randomForest (Liaw and Wiener, 2002)
	mtry	Number of variables selected at each split	[4, 6, 8]	
XGBoost	nrounds	Maximum number of boosting rounds	[100, 500, 1000]	xgboost (Chen et al., 2024)
	max_depth	Maximum depth of a tree	[4, 6, 8]	
	eta	Learning rate	[0.01, 0.3, 0.5]	
RFE	method	External resampling method	cross-validation	caret (Kuhn, 2008)
	number	Number of folds/ resampling iterations	5	
Train/test split		Random split of observations into training and test data	[0.7, 0.75, 0.8]	

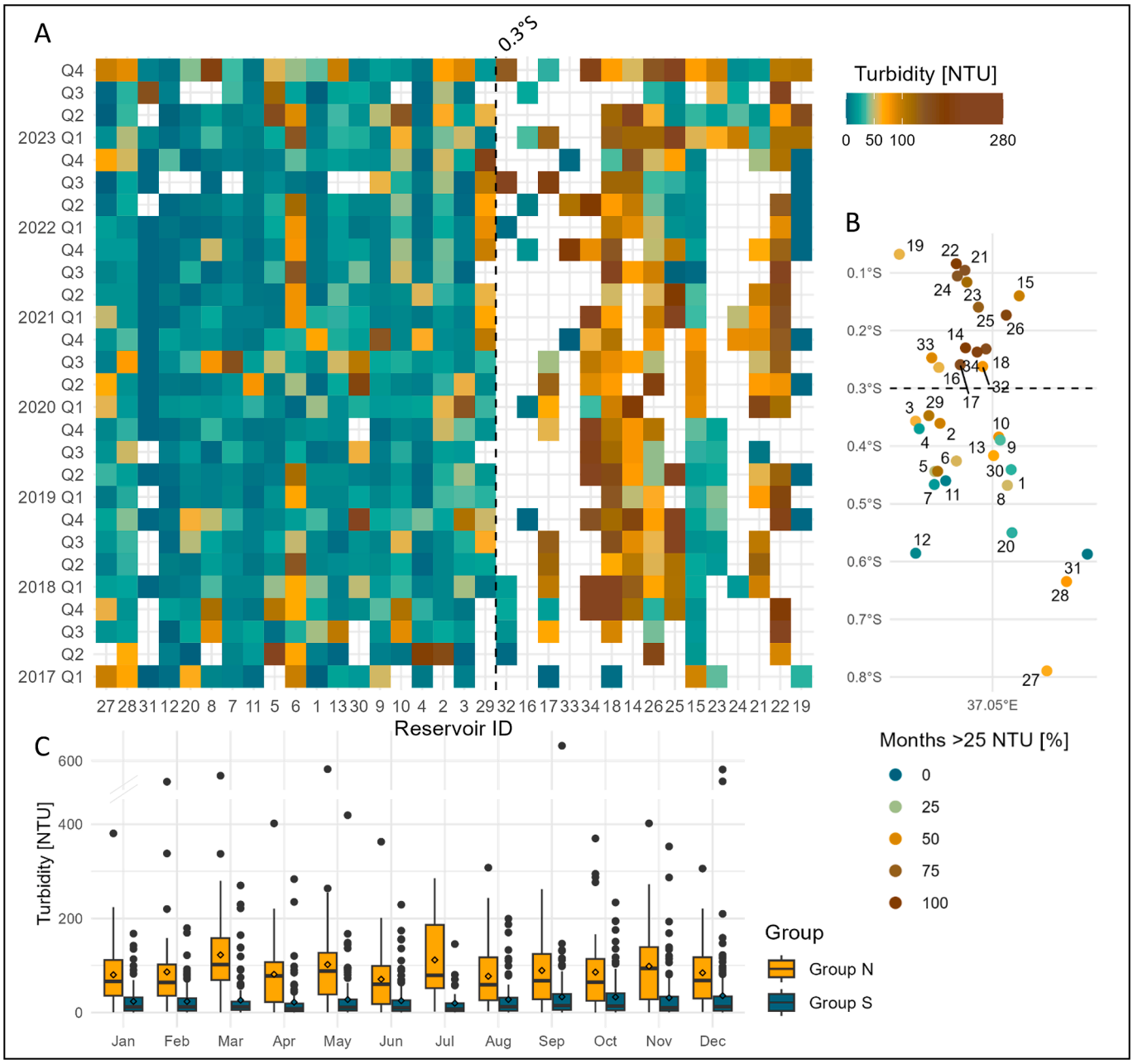

Fig. 3. A Quarterly averaged turbidity from south to north (left to right), B months > 25 NTU (percentage), and C interquartile range plots for groups north and south of 0.3°S. The dashed line in A and B separates Group N and S.

land management and land cover predictors had the largest share for both models with 78.0 % for RF and 94.1 % for XGBoost. 5 km WUI was the most important predictor for both, followed by land cover predictors at the 5 km and catchment scale. The maxima of windspeed and rainfall ranked higher than the mean and sum, with the exception of rainfall sum that had a slightly higher importance compared to its maximum for XGBoost. While slope and water volume had intermediate and low importance for RF, their contribution was almost insignificant in the XGBoost model.

5. Discussion

5.1. Turbidity dynamics and predictor importance

Turbidity derived from Sentinel-2 images is a scalable proxy for detecting water quality patterns and changes (Warren et al., 2021). Turbidity in the study area shows seasonality when clustered into groups. However, it is not as distinct as in previous spatio-temporal studies that largely attributed turbidity variability in water bodies to seasonal meteorological parameters (Zhang et al., 2021). Other studies have also integrated land cover indicators and retrieved markedly seasonal patterns (Shen et al., 2022). However, the studied water bodies were much larger than those here, which reflects more the findings by Robert et al. (2017), where spatial and temporal patterns are observable, but less straightforwardly linked to seasonal drivers. The marked difference in turbidity between Group N and S indicates that the conditions that influence turbidity change along a north–south axis. While Group S has low turbidity levels from March to May and in July, Group N shows high levels in April and July. The first rainy season from March to May entails a vegetation green-up, which likely mitigates part of the erosion and sediment input for Group S but is not pronounced enough in the study area's dryer, less vegetated northern part. Likewise, the annual

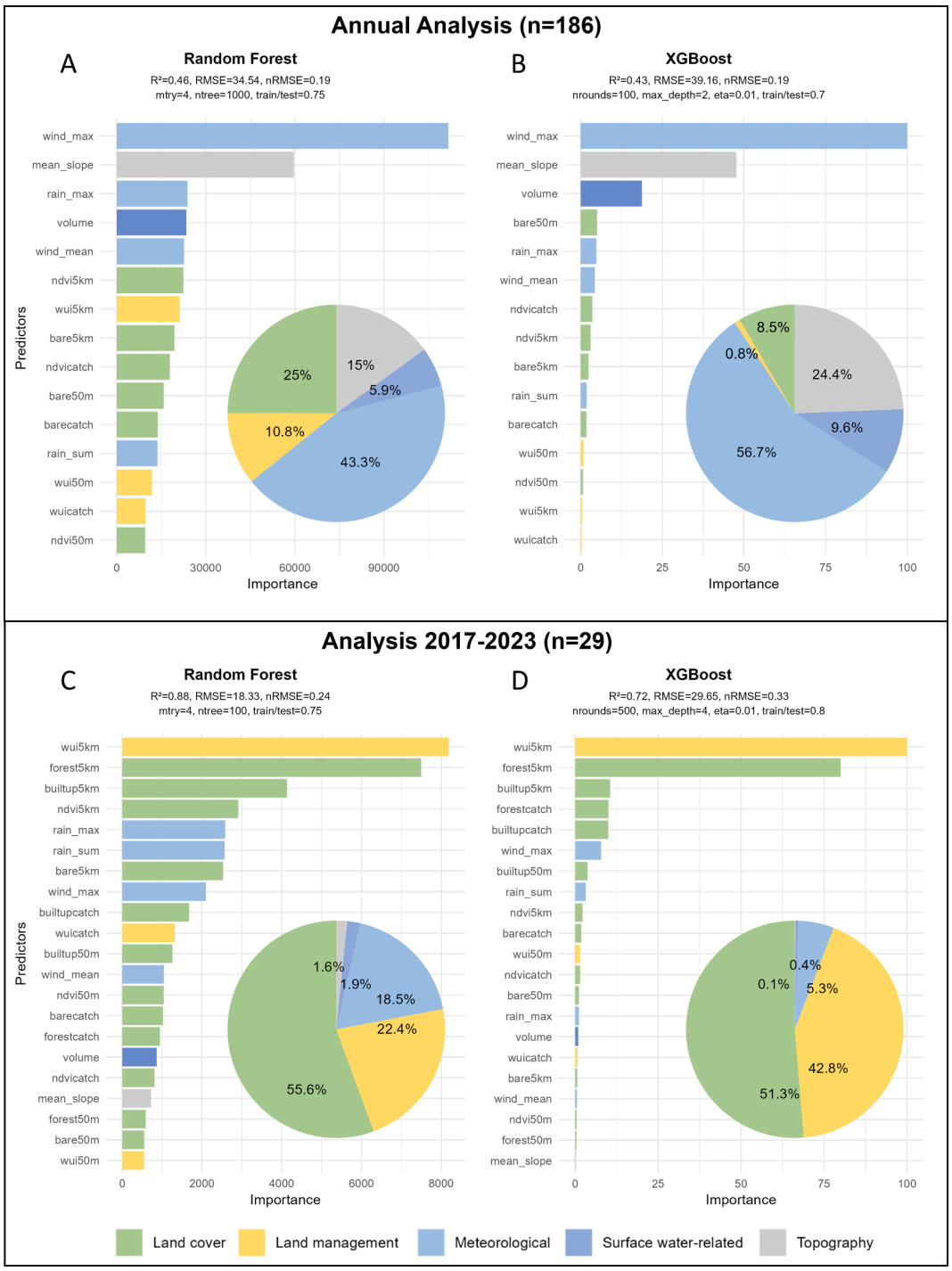

Fig. 4. Median of RFE-selected variable importances for annual (A, B) and long-term analyses 2017–2023 (C, D), median model performances, and most frequently selected hyperparameter combinations of the respective best-performing model. Variable importance is measured as decrease in impurity for RF and gain for XGBoost.

maximum windspeed around July seems to impact turbidity more in Group N. Shen et al. (2022) detected clear water in the smaller of their studied lakes and attributed this to less area being affected by wind. In contrast, we found high turbidity in the reservoirs and identified maximum windspeed as an important predictor. Group N is located on higher and flatter terrain with less vegetation cover to act as windbreaks and is therefore likely more affected than Group S.

While windspeed and rainfall maxima still have intermediate importance in the longer-term analysis, land management and cover become the most important predictors. This may be because they are able to reflect the complex interactions between environmental and anthropogenic factors in the long run. While weather extremes impact inter-annual turbidity, long-term turbidity patterns seem to be related more to which management and land planning strategies are taken. WUI captures the magnitude and frequency of changes on the land surface, induced for example by ploughing, vegetation greening, harvesting, de- or reforestation, and therefore appears to perform particularly well for longer-term analysis. Land management and cover predictors at the 5 km and catchment scale both tend to have high importance, confirming the finding by Cecchi et al. (2020). However, small buffers that account

for riparian and other vegetation, or the lack thereof, near the water body proved to be of relevance, although to a lesser degree. To define more meaningful thresholds, breakpoint analysis could help find suitable buffer distances (c.f. Locke and Winter, 2024). The results confirm that previously published predictors, usually used for larger water bodies, also played a role in small reservoirs. The lower predictive power of the annual models suggests that short-term management actions directly on the reservoirs, such as pumping, dredging, timing of livestock watering, and herd sizes play a particularly important role in small water bodies. Quantitative information on the frequency and scope of these actions could improve the prediction.

5.2. Implications for sustainable water resources management

The study used freely available primary and secondary data. The DEM is the only exception and could be replaced with an alternative. Turbidity was processed with free and open software and without additional in-situ data collection. Although the model was already adjusted to the study area by Steinbach et al. (2024), they show that relative turbidity dynamics are also captured well by the C2RCC model if it is not optimally parameterized. This makes the approach transferrable and applicable, which is particularly important for small water bodies with no available in-situ information. However, several technical challenges exist. Missing observations cause gaps in the time series. Also, adjacency effects are inevitable in small water bodies. We mitigated these by selecting observations from a centre location in each reservoir, but this location may not be representative of where users withdraw water. Quality flagging, supported by the water presence time series, and a more individual choice of data retrieval points could improve the results' relevance (e.g., Jiang et al., 2023; Lehmann et al., 2021).

Our results show that the critical KEBS threshold was exceeded regularly in most of the reservoirs, with possible negative impacts on human and livestock health, crops, irrigation equipment, and aquaculture, and increased risk of rapid siltation (Saruchera and Lautze, 2019). These can be expected for most reservoirs in the study area, where Group N is more affected. Identifying the most important influencing factors helps finding the most effective management levers. Thus, measures that reduce deflation could be of particular interest in the northern part of the study area. In contrast, water volume influences intra-annual turbidity variability but may be difficult to control if water levels depend on rainfall and extraction on need. It could, however, be integrated at the planning and construction stage. The presented workflow could furthermore be used for scenario-building under changing climate and land use. A challenge lies in the interpretation of the predictor-turbidity relationship and in the interrelations between different predictors, which requires knowledge of the local land and water management systems. Including socio-hydrological information, such as timing and purpose of water extraction, maintenance, ownership, access restrictions, and governance structures (c.f. Ogilvie et al., 2019), would further help contextualising interlinkages between water quantity, quality, and use.

6. Conclusions

In this study, we modelled turbidity with Sentinel-2 imagery and C2RCC in small reservoirs at monthly, annual, and multi-annual scale and estimated the impact of predictors on inter- and multi-annual variability. We could identify partly contrasting turbidity patterns in the southern and northern reservoir clusters, where many reservoirs exceeded safe levels regularly. With maximum windspeed being the most important predictor according to RF and XGBoost, weather patterns strongly affected inter-annual turbidity variability, whereas land management and land cover influenced longer-term turbidity outcomes. These analyses combined are useful to understand the spatio-temporal relationships between environmental and weather-related factors and turbidity. Our results demonstrate the capacity of an approach with free data and tools, combined with machine learning, to assess and monitor turbidity. Such comprehensive, spatial and temporal knowledge can support targeted reservoir siting and informed water and land management decisions. Moreover, applying this approach to other sites across SSA can help advance the knowledge basis on overall water quality and its dynamics in small water bodies.

CRediT authorship contribution statement

Stefanie Steinbach: Writing – review & editing, Writing – original draft, Visualization, Methodology, Investigation, Formal analysis, Data curation, Conceptualization. **Anna Bartels:** Writing – review & editing, Formal analysis. **Andreas Rienow:** Writing – review & editing, Resources, Project administration. **Bartholomew Thiong'o Kuria:** Writing – review & editing, Project administration. **Sander Jaap Zwart:** Writing – review & editing, Supervision, Methodology, Conceptualization. **Andrew Nelson:** Writing – review & editing, Supervision, Methodology, Conceptualization.

Declaration of competing interest

The authors declare that they have no known competing financial interests or personal relationships that could have appeared to influence the work reported in this paper.

Acknowledgements

This work was supported by the German Federal Ministry of Education and Research (BMBF) through the Project "Participatory Approach to Environmental Conservation of the Muringato Catchment Area for Sustainable Management and Enhanced Ecosystem Health" (CITGI4Muringato) under Grant Agreement No. 01DG20022. The authors would like to acknowledge the German Aerospace Center (DLR) for providing the TanDEM-X DEM for the study area. We thank Torben Dedring for providing technical support with data processing on the server.

Data availability

S1, S2: Copernicus Dataspace (dataspace.copernicus.eu), S1, S2, CHIRPS, ERA5: GEE (developers.google.com/earth-engine/datasets). WUI: Steinbach et al. (2023). Scripts: doi.org/10.5281/zenodo.14245504.

References

Bangira, T., Alfieri, S.M., Menenti, M., Van Niekerk, A., 2019. Comparing thresholding with machine learning classifiers for mapping complex water. Remote Sens. 11, 1351. https://doi.org/10.3390/rs11111351.

Bhaga, T.D., Dube, T., Shekede, M.D., Shoko, C., 2023. Investigating the effectiveness of Landsat-8 OLI and Sentinel-2 MSI satellite data in monitoring the effects of drought on surface water resources in the Western Cape Province, South Africa. Remote Sens. Appl. Soc. Environ. 32, 101037. https://doi.org/10.1016/j.rsase.2023.101037.

Breiman, L., 2001. Random Forests. Mach. Learn. 45, 5–32. https://doi.org/10.1023/A:1010933404324.

Brockmann, C., Doerffer, R., Peters, M., Stelzer, K., Embacher, S., Ruescas, A., 2016. Evolution of the C2RCC Neural Network for Sentinel 2 and 3 for the Retrieval of Ocean Colour Products in Normal and Extreme Optically Complex Waters, in: *Proceedings*. Presented at the Living Planet Symposium, ESA-SP, Prague, Czech Republic, p. 54.

Cecchi, P., Forkuor, G., Cofie, O., Lalanne, F., Poussin, J.-C., Jamin, J.-Y., 2020. Small Reservoirs, landscape changes and water quality in sub-saharan west africa. Water 12, 1967. https://doi.org/10.3390/w12071967.

Chen, T., He, T., Benesty, M., Khotilovich, V., Tang, Y., Cho, H., Chen, K., Mitchell, R., Cano, I., Zhou, T., Li, M., Xie, J., Lin, M., Geng, Y., Li, Y., Yuan, J., 2024. xgboost: eXtreme Gradient Boosting, 2024. (Version 1.7.7.1) [software] https://CRAN.R-project.org/package=xgboost.

Copernicus Climate Change Service, 2019. ERA5-Land monthly averaged data from 2001 to present. https://doi.org/10.24381/CDS.68D2BB30.

Davies-Colley, R.J., Smith, D.G., 2001. Turbidity, suspended sediment, and water clarity: A review. JAWRA J. Am. Water Resour. Assoc. 37, 1085–1101. https://doi.org/10.1111/j.1752-1688.2001.tb03624.x.

De Troyer, N., Mereta, S., Goethals, P., Boets, P., 2016. Water quality assessment of streams and wetlands in a fast growing east african city. Water 8, 123. https://doi.org/10.3390/w8040123.

Defersha, M.B., Melesse, A.M., 2012. Effect of rainfall intensity, slope and antecedent moisture content on sediment concentration and sediment enrichment ratio. Catena 90, 47–52. https://doi.org/10.1016/j.catena.2011.11.002.

Díaz-Uriarte, R., Alvarez De Andrés, S., 2006. Gene selection and classification of microarray data using random forest. BMC Bioinf. 7, 3. https://doi.org/10.1186/1471-2105-7-3.

Dörnhöfer, K., Oppelt, N., 2016. Remote sensing for lake research and monitoring – Recent advances. Ecol. Indic. 64, 105–122. https://doi.org/10.1016/j.ecolind.2015.12.009.

ESA, 2022. SNAP - ESA Sentinel Application Platform, 2022. (Version 9.0) [software]. http://step.esa.int/.

Funk, C., Peterson, P., Landsfeld, M., Pedreros, D., Verdin, J., Shukla, S., Husak, G., Rowland, J., Harrison, L., Hoell, A., Michaelsen, J., 2015. The climate hazards infrared precipitation with stations—a new environmental record for monitoring extremes. Sci. Data 2, 150066. https://doi.org/10.1038/sdata.2015.66.

Gardelle, J., Hiernaux, P., Kergoat, L., Grippa, M., 2010. Less rain, more water in ponds: a remote sensing study of the dynamics of surface waters from 1950 to present in pastoral Sahel (Gourma region, Mali). Hydrol. Earth Syst. Sci. 14, 309–324. https://doi.org/10.5194/hess-14-309-2010.

Ghansah, B., Foster, T., Higginbottom, T.P., Adhikari, R., Zwart, S.J., 2022. Monitoring spatial-temporal variations of surface areas of small reservoirs in Ghana's Upper East Region using Sentinel-2 satellite imagery and machine learning. Phys. Chem. Earth Parts ABC 125, 103082. https://doi.org/10.1016/j.pce.2021.103082.

Goebel, M., Thiong'o, K., Rienow, A., 2023. Object-based mapping and classification features for tropical highlands using Sentinel-2, Sentinel-2, and GEDI Canopy Height data - A case study of the Muringato Catchment, Kenya. *Erdkunde 77*, 35–52. https://doi.org/10.3112/erdkunde.2023.01.03.

Gorelick, N., Hancher, M., Dixon, M., Ilyushchenko, S., Thau, D., Moore, R., 2017. Google Earth Engine: Planetary-scale geospatial analysis for everyone. Remote Sens. Environ. 202, 18–27. https://doi.org/10.1016/j.rse.2017.06.031.

Hampel, F.R., 1974. The Influence Curve and its Role in Robust Estimation. J. Am. Stat. Assoc. 69, 383–393. https://doi.org/10.1080/01621459.1974.10482962.

Henley, W.F., Patterson, M.A., Neves, R.J., Lemly, A.D., 2000. Effects of Sedimentation and Turbidity on Lotic Food Webs: A Concise Review for Natural Resource Managers. Rev. Fish. Sci. 8, 125–139. https://doi.org/10.1080/10641260091129198.

Jiang, D., Scholze, J., Liu, X., Simis, S.G.H., Stelzer, K., Müller, D., Hunter, P., Tyler, A., Spyrakos, E., 2023. A data-driven approach to flag land-affected signals in satellite derived water quality from small lakes. Int. J. Appl. Earth Obs. Geoinformation 117, 103188. https://doi.org/10.1016/j.jag.2023.103188.

Kauffman, S., Droogers, P., Hunink, J., Mwaniki, B., Muchena, F., Gicheru, P., Bindraban, P., Onduru, D., Cleveringa, R., Bouma, J., 2014. Green Water Credits – exploring its potential to enhance ecosystem services by reducing soil erosion in the Upper Tana basin. Kenya. *Int. J. Biodivers. Sci. Ecosyst. Serv. Manag.* 10, 133–143. https://doi.org/10.1080/21513732.2014.890670.

Kebs, 2015. Kenya Standard (KS EAS 12: 2014, First Edition. Specifications for potable water, Kenya Bureau of Standards (KEBS), Nairobi, Kenya. https://academicjournals.org/journal/IJWREE/article-full-text-pdf/03934C661299 (accessed 15-6-2023.

Kibret, S., McCartney, M., Lautze, J., Nhamo, L., Yan, G., 2021. The impact of large and small dams on malaria transmission in four basins in Africa. Sci. Rep. 11, 13355. https://doi.org/10.1038/s41598-021-92924-3.

Kowe, P., Ncube, E., Magidi, J., Ndambuki, J.M., Rwasoka, D.T., Gumindoga, W., Maviza, A., De Jesus Paulo Mavaringana, M., Kakanda, E.T., 2023. Spatial-temporal variability analysis of water quality using remote sensing data: A case study of Lake Manyame. *Sci. Afr. 21*, e01877. https://doi.org/10.1016/j.sciaf.2023.e01877.

Kuhn, M., 2008. Building Predictive Models in R Using the caret Package. J. Stat. Softw. 28. https://doi.org/10.18637/jss.v028.i05.

Lacour, C., Joannis, C., Gromaire, M.-C., Chebbo, G., 2009. Potential of turbidity monitoring for real time control of pollutant discharge in sewers during rainfall events. Water Sci. Technol. 59, 1471–1478. https://doi.org/10.2166/wst.2009.169.

Lehmann, M.K., Schütt, E.M., Hieronymi, M., Dare, J., Krasemann, H., 2021. Analysis of recurring patchiness in satellite-derived chlorophyll a to aid the selection of representative sites for lake water quality monitoring. Int. J. Appl. Earth Obs. Geoinformation 104, 102547. https://doi.org/10.1016/j.jag.2021.102547.

Liaw, A., Wiener, M., 2002. Classification and Regression by randomForest. R News 2, 18–22. https://journal.r-project.org/articles/RN-2002-022/RN-2002-022.pdf.

Lin, X., Wu, M., Shao, X., Li, G., Hong, Y., 2023. Water turbidity dynamics using random forest in the Yangtze River Delta Region. China. *Sci. Total Environ.* 903, 166511. https://doi.org/10.1016/j.scitotenv.2023.166511.

Liu, D., Duan, H., Loiselle, S., Hu, C., Zhang, G., Li, J., Yang, H., Thompson, J.R., Cao, Z., Shen, M., Ma, R., Zhang, M., Han, W., 2020. Observations of water transparency in China's lakes from space. Int. J. Appl. Earth Obs. Geoinformation 92, 102187. https://doi.org/10.1016/j.jag.2020.102187.

Locke, K.A., 2024. Impacts of land use/land cover on water quality: a contemporary review for researchers and policymakers. Water Qual. Res. J. wqrj2024002. https://doi.org/10.2166/wqrj.2024.002.

Locke, K.A., Winter, K., 2024. Estimating thresholds of natural vegetation for the protection of water quality in South African catchments. Sci. Total Environ. 945, 173924. https://doi.org/10.1016/j.scitotenv.2024.173924.

Martins, V.S., Kaleita, A., Barbosa, C.C.F., Fassoni-Andrade, A.C., Lobo, F.D.L., Novo, E. M.L.M., 2019. Remote sensing of large reservoir in the drought years: Implications on surface water change and turbidity variability of Sobradinho reservoir (Northeast Brazil). Remote Sens. Appl. Soc. Environ. 13, 275–288. https://doi.org/10.1016/j.rsase.2018.11.006.

Masocha, M., Dube, T., Nhiwatiwa, T., Choruma, D., 2018. Testing utility of Landsat 8 for remote assessment of water quality in two subtropical African reservoirs with contrasting trophic states. Geocarto Int. 33, 667–680. https://doi.org/10.1080/10106049.2017.1289561.

Müller, K., Cornel, P., 2017. Setting water quality criteria for agricultural water reuse purposes. J. Water Reuse Desalination 7, 121–135. https://doi.org/10.2166/wrd.2016.194.

Muringato Water Resource Users Association (WRUA), 2018. Report on the baseline mapping and documentation of Muringato WRUA sub-catchment characteristics - Basic inventory. Dedan Kimathi University of Technology, Nyeri, Kenya.

Muthee, S.W., Kuria, B.T., Mundia, C.N., Sichangi, A.W., Kuria, D.N., Goebel, M., Rienow, A., 2022. Using SWAT to model the response of evapotranspiration and runoff to varying land uses and climatic conditions in the Muringato basin, Kenya. *Model. Earth Syst. Environ.* https://doi.org/10.1007/s40808-022-01579-0.

Mwaura, F., 2006. Some aspects of water quality characteristics in small shallow tropical man-made reservoirs in Kenya. Afr. J. Sci. Technol. 7, 82–96. https://doi.org/10.4314/ajst.v7i1.55203.

Nakawuka, P., Langan, S., Schmitter, P., Barron, J., 2018. A review of trends, constraints and opportunities of smallholder irrigation in East Africa. Glob. Food Secur. 17, 196–212. https://doi.org/10.1016/j.gfs.2017.10.003.

Nathan, O.O., Felix, N.K., Milka, K.N., Anne, M., Noah, A., Daniel, M.N., 2020. Suitability of different data sources in rainfall pattern characterization in the tropical central highlands of Kenya. Heliyon 6, e05375.

Ndou, N., 2023. Geostatistical inference of Sentinel-2 spectral reflectance patterns to water quality indicators in the Setumo dam, South Africa. Remote Sens. Appl. Soc. Environ. 30, 100945. https://doi.org/10.1016/j.rsase.2023.100945.

Ogilvie, A., Riaux, J., Massuel, S., Mulligan, M., Belaud, G., Le Goulven, P., Calvez, R., 2019. Socio-hydrological drivers of agricultural water use in small reservoirs. Agric. Water Manag. 218, 17–29. https://doi.org/10.1016/j.agwat.2019.03.001.

Otsu, N., 1979. A Threshold Selection Method from Gray-Level Histograms. IEEE Trans. Syst. Man Cybern. 9, 62–66. https://doi.org/10.1109/TSMC.1979.4310076.

Papa, F., Crétaux, J.-F., Grippa, M., Robert, E., Trigg, M., Tshimanga, R.M., Kitambo, B., Paris, A., Carr, A., Fleischmann, A.S., De Fleury, M., Gbetkom, P.G., Calmettes, B., Calmant, S., 2023. Water Resources in Africa under Global Change: monitoring surface waters from space. Surv. Geophys. 44, 43–93. https://doi.org/10.1007/s10712-022-09700-9.

Pichler, M., Hartig, F., 2023. Machine learning and deep learning—A review for ecologists. Methods Ecol. Evol. 14, 994–1016. https://doi.org/10.1111/2041-210X.14061.

Potapov, P., Li, X., Hernandez-Serna, A., Tyukavina, A., Hansen, M.C., Kommareddy, A., Pickens, A., Turubanova, S., Tang, H., Silva, C.E., Armston, J., Dubayah, R., Blair, J. B., Hofton, M., 2021. Mapping global forest canopy height through integration of GEDI and Landsat data. Remote Sens. Environ. 253, 112165. https://doi.org/10.1016/j.rse.2020.112165.

R Core Team, 2024. R: A Language and Environment for Statistical Computing, 2024. (Version 4.4.1) [software]. https://www.R-project.org/.

Rizzoli, P., Martone, M., Gonzalez, C., Wecklich, C., Borla Tridon, D., Bräutigam, B., Bachmann, M., Schulze, D., Fritz, T., Huber, M., Wessel, B., Krieger, G., Zink, M., Moreira, A., 2017. Generation and performance assessment of the global TanDEM-X digital elevation model. ISPRS J. Photogramm. Remote Sens. 132, 119–139. https://doi.org/10.1016/j.isprsjprs.2017.08.008.

Robert, E., Grippa, M., Kergoat, L., Pinet, S., Gal, L., Cochonneau, G., Martinez, J.-M., 2016. Monitoring water turbidity and surface suspended sediment concentration of the Bagre Reservoir (Burkina Faso) using MODIS and field reflectance data. Int. J. Appl. Earth Obs. Geoinformation 52, 243–251. https://doi.org/10.1016/j.jag.2016.06.016.

Robert, E., Kergoat, L., Soumaguel, N., Merlet, S., Martinez, J.-M., Diawara, M., Grippa, M., 2017. Analysis of Suspended Particulate matter and its drivers in sahelian ponds and lakes by remote sensing (Landsat and MODIS): Gourma Region. Mali. *Remote Sens.* 9, 1272. https://doi.org/10.3390/rs9121272.

Sagan, V., Peterson, K.T., Maimaitijiang, M., Sidike, P., Sloan, J., Greeling, B.A., Maalouf, S., Adams, C., 2020. Monitoring inland water quality using remote sensing: potential and limitations of spectral indices, bio-optical simulations, machine learning, and cloud computing. Earth-Sci. Rev. 205, 103187. https://doi.org/10.1016/j.earscirev.2020.103187.

Saruchera, D., Lautze, J., 2019. Small reservoirs in Africa: a review and synthesis to strengthen future investment. International Water Management Institute (IWMI). https://doi.org/10.5337/2019.209.

Shen, M., Cao, Z., Xue, K., Liu, D., Qi, T., Ma, J., Duan, H., 2022. Natural and human activities driving the spatiotemporal variability of water clarity in lakes across Eastern China. Int. J. Appl. Earth Obs. Geoinformation 114, 103037. https://doi.org/10.1016/j.jag.2022.103037.

Soriano-González, J., Urrego, E.P., Sòria-Perpinyà, X., Angelats, E., Alcaraz, C., Delegido, J., Ruíz-Verdú, A., Tenjo, C., Vicente, E., Moreno, J., 2022. Towards the Combination of C2RCC Processors for Improving Water Quality Retrieval in Inland and Coastal Areas. Remote Sens. 14, 1124. https://doi.org/10.3390/rs14051124.

Steinbach, S., Cornish, N., Franke, J., Hentze, K., Strauch, A., Thonfeld, F., Zwart, S.J., Nelson, A., 2021. A New Conceptual Framework for integrating earth observation in large-scale wetland management in east africa. Wetlands 41, 93. https://doi.org/10.1007/s13157-021-01468-9.

Steinbach, S., Rienow, A., Chege, M.W., Dedring, N., Kipkemboi, W., Thiong'o, B.K., Zwart, S.J., Nelson, A., 2024. Low-Cost Sensors and Multitemporal Remote Sensing for Operational Turbidity Monitoring in an East African Wetland Environment. *IEEE*

J. Sel. Top. Appl. Earth Obs. Remote Sens. 17, 8490–8508. https://doi.org/10.1109/JSTARS.2024.3381756.

Steinbach, S., Hentschel, E., Hentze, K., Rienow, A., Umulisa, V., Zwart, S.J., Nelson, A., 2023. Automatization and evaluation of a remote sensing-based indicator for wetland health assessment in East Africa on national and local scales. Ecol. Inform. 75, 102032. https://doi.org/10.1016/j.ecoinf.2023.102032.

Tucker, C.J., 1979. Red and photographic infrared linear combinations for monitoring vegetation. Remote Sens. Environ. 8, 127–150. https://doi.org/10.1016/0034-4257(79)90013-0.

Urbina-Salazar, D., Vaudour, E., Richer-de-Forges, A.C., Chen, S., Martelet, G., Baghdadi, N., Arrouays, D., 2023. Sentinel-2 and Sentinel-1 Bare soil temporal mosaics of 6-year periods for soil organic carbon content mapping in central france. Remote Sens. 15, 2410. https://doi.org/10.3390/rs15092410.

Uwimana, A., van Dam, A.A., Irvine, K., 2018. Effects of conversion of wetlands to rice and fish farming on water quality in valley bottoms of the Migina catchment, southern Rwanda. Ecol. Eng. 125, 76–86. https://doi.org/10.1016/j.ecoleng.2018.10.019.

Vanthof, V., Kelly, R., 2019. Water storage estimation in ungauged small reservoirs with the TanDEM-X DEM and multi-source satellite observations. Remote Sens. Environ. 235, 111437. https://doi.org/10.1016/j.rse.2019.111437.

Wang, X., Song, K., Wen, Z., Liu, G., Shang, Y., Fang, C., Lyu, L., Wang, Q., 2021. Quantifying turbidity variation for lakes in daqing of northeast china using landsat images From 1984 to 2018. *IEEE J.* Sel. Top. Appl. Earth Obs. Remote Sens. 14, 8884–8897. https://doi.org/10.1109/JSTARS.2021.3101475.

Warren, M.A., Simis, S.G.H., Selmes, N., 2021. Complementary water quality observations from high and medium resolution Sentinel sensors by aligning chlorophyll-a and turbidity algorithms. Remote Sens. Environ. 265, 112651. https://doi.org/10.1016/j.rse.2021.112651.

Winton, R.S., Calamita, E., Wehrli, B., 2019. Reviews and syntheses: dams, water quality and tropical reservoir stratification. Biogeosciences 16, 1657–1671. https://doi.org/10.5194/bg-16-1657-2019.

Yin, F., Lewis, P.E., Gómez-Dans, J.L., 2022. Bayesian atmospheric correction over land: Sentinel-2/MSI and Landsat 8/OLI. Geosci. Model Dev. 15, 7933–7976. https://doi.org/10.5194/gmd-15-7933-2022.

Zhang, L., Xin, Z., Feng, L., Hu, C., Zhou, H., Wang, Y., Song, C., Zhang, C., 2022. Turbidity dynamics of large lakes and reservoirs in northeastern China in response to natural factors and human activities. J. Clean. Prod. 368, 133148. https://doi.org/10.1016/j.jclepro.2022.133148.

Zhang, Y., Yao, X., Wu, Q., Huang, Y., Zhou, Z., Yang, J., Liu, X., 2021. Turbidity prediction of lake-type raw water using random forest model based on meteorological data: a case study of Tai lake. China. *J. Environ. Manage.* 290, 112657. https://doi.org/10.1016/j.jenvman.2021.112657.